CASE REPORT

Subclinical Capillary Changes in Non-Proliferative Diabetic Retinopathy

Johnny Tam*, Kavita P. Dhamdhere†, Pavan Tiruveedhula‡, Brandon J. Lujan†, Robert N. Johnson†, Marcus A. Bearse, Jr.*, Anthony J. Adams§, and Austin Roorda*

ABSTRACT

Purpose. To establish adaptive optics scanning laser ophthalmoscopy as a method to detect and characterize microscopic signs of diabetic retinopathy in capillaries and cone photoreceptors in the parafovea.

Methods. Recently, adaptive optics scanning laser ophthalmoscope (AOSLO) has enabled noninvasive assessment of photoreceptors, capillaries, and leukocytes in the retinas of live human subjects. Repeated application of AOSLO imaging along with comparison to fluorescein angiography was used to track individual capillaries near the foveal avascular zone (FAZ) from one eye affected with severe non-proliferative diabetic retinopathy. Fluorescein angiography was used to identify clinical signs of diabetic retinopathy, such as microaneurysms and intraretinal microvascular abnormalities, and corresponding regions were imaged and assessed using the AOSLO. In addition, the structural integrity of photoreceptors and the spatial distribution of leukocytes around the parafoveal capillary network were quantitatively assessed.

Results. Capillaries and cone photoreceptors were visualized using the AOSLO without the use of injected contrast agents. Although the majority of capillaries were stable over a period of 16 months, one capillary at the edge of the FAZ dropped out, leading to a small but significant increase in FAZ size. Longitudinal assessment of the capillaries also showed microaneurysm formation and disappearance as well as the formation of tiny capillary bends similar in appearance to intraretinal microvascular abnormalities. The leukocytes in the capillary network were found to preferentially travel through the same routes in all four visits, suggesting that these channels are robust against small changes to the surrounding capillaries. In this eye, cone photoreceptor spacing was increased in the fovea when compared with normal data but stable across all visits.

Conclusions. AOSLO imaging can be used to longitudinally track capillaries, leukocytes, and photoreceptors in diabetic retinopathy. Capillary changes that can be detected include dropout of individual capillaries as well as formation and disappearance of microaneurysms.
(Optom Vis Sci 2012;89:E692–E703)

Key Words: adaptive optics, capillaries, diabetic retinopathy, leukocyte, microaneurysm, photoreceptors

Diabetes is a systemic disease that affects many different tissues and organs including the eye. In the retina, the corresponding disease is called diabetic retinopathy (DR) which can lead to blindness if untreated. Signs of DR are present in nearly all patients who have had type 1 diabetes for two decades.[1] The first stage of DR, non-proliferative DR (NPDR), is marked by gradual capillary dropout. Associated with NPDR are a set of clinically observable changes in the microcirculation, which include microaneurysms (MAs), or small outpouchings of the capillary wall, and intraretinal microvascular abnormalities (IRMAs), which are focal disruptions of the capillary topology.

These clinically observable changes are noticeable mainly because they are larger in size than the surrounding capillaries. For example, fundus photography is a non-invasive method to detect MAs visible as small dots. New dots appear and existing dots disappear over time,[2] presumably due to formation of new outpouchings and non-perfusion of existing outpouchings. However, using fundus photography, it is not possible to investigate the relationship of MAs to the surrounding capillaries. This is because it is
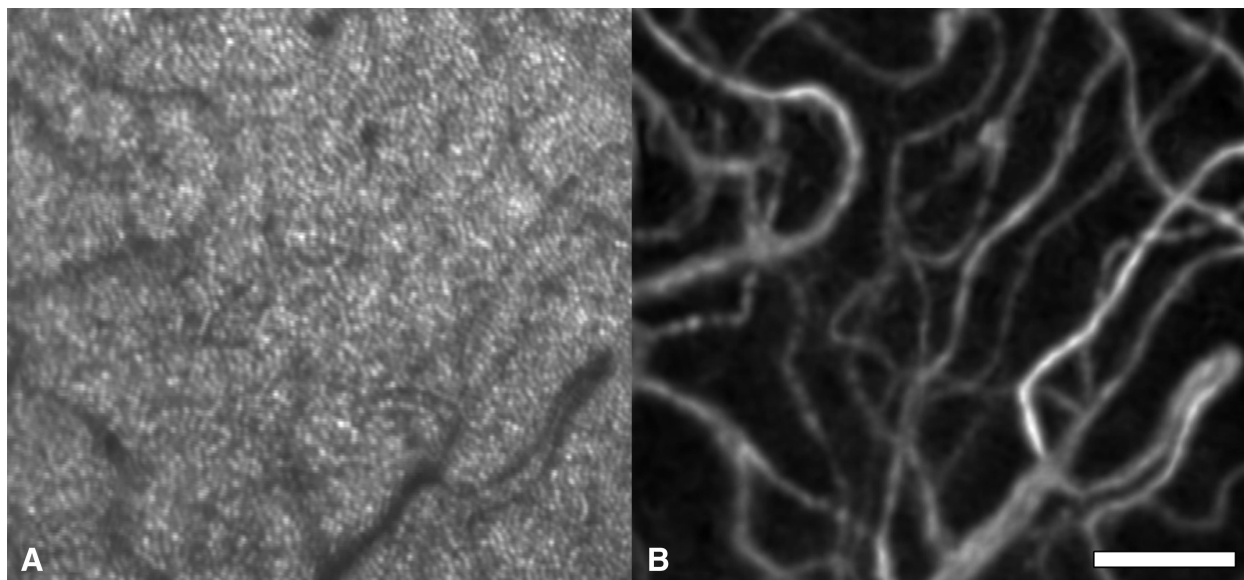
FIGURE 1.

High-resolution images of a live human retina generated using an adaptive optics scanning laser ophthalmoscope (AOSLO). Both images were generated noninvasively from the same AOSLO video. (A) This image was generated by averaging frames across the video. Small circular dots are cone photoreceptors. Dark, fuzzy lines generally correspond to capillaries; however, in many areas, the spatial contrast is low, making it difficult to determine the location of the capillaries. (B) Image of capillaries generated using intrinsic motion contrast signals without the use of injected contrast agents. Scale bar, 100 μm.

difficult to image capillaries due to their small size and low contrast. We have recently developed a technique based on an adaptive optics scanning laser ophthalmoscope (AOSLO) that can noninvasively generate detailed images of capillaries without the use of injected dyes; this method is based on the use of motion as an intrinsic contrast signal[3–5] (Fig. 1 and Supplemental Digital Content 1 available online at http://links.lww.com/OPX/A87). There are currently several other methods for the non-invasive investigation of capillaries based on fundus photography[6] and phase variance optical coherence tomography.[7,8] Although the AOSLO has been used to evaluate retinal blood flow,[9,10] it is not yet established whether AOSLO imaging can detect capillary defects such as MAs or IRMAs.

The gold standard for investigating human retinal capillaries is fluorescein angiography (FA). There are clear advantages for using FA to evaluate DR. These include the improved ability to detect MAs as well as the ability to assess regions of capillary dropout or capillary remodeling. Studies using FA-based methods have shown increases in both the size of the foveal avascular zone (FAZ) and the areas of the perifoveal intercapillary areas.[11,12] Fluorescein has also been used to investigate blood flow in humans; in diabetes, the speed of capillary blood flow is decreased.[13] FA has been combined with AOSLO imaging,[14] but thus far, this method has not been applied to study DR. Typically, FA is performed by injecting a bolus of fluorescein dye into a peripheral vein and then imaging the passage of the dye using a fundus camera. However, administration of fluorescein dye is clinically indicated only in the later stages of DR. As with all invasive procedures, there is also a small risk of adverse side effects.[15] There have been many efforts to develop instruments to image the capillaries, to assess the early stages of DR, and to investigate other retinal diseases.

In this article, we establish that AOSLO can be used to detect both clinical and subclinical signs of DR in the retina, where clin-ical signs are retinal features that would be considered to be clinically significant (e.g., MAs and IRMAs) and subclinical signs are retinal features that would not be considered clinically significant by the current standards of care (e.g., capillary bends and cone photoreceptor spacing). We use the AOSLO to simultaneously assess photoreceptors, capillaries, and leukocytes.

METHODS

Study Design

We invited a 26-year-old male subject with type 1 diabetes and severe NPDR to participate in a series of imaging and assessment visits to determine whether we could detect any capillary changes as well as any signs of capillary dropout. Detection of capillary dropout is most likely during severe NPDR, because the next stage of the disease, proliferative DR, is marked by neovascularization. To maximize the sensitivity with which changes to the capillaries could be detected, we performed all the assessments in the same eye. This eliminates the need to consider intersubject variability which is large in the retinal microcirculation.[16] To assess the capillaries, we used a method based on AOSLO imaging that enables the generation of highly detailed capillary images. In addition, we also performed conventional clinical tests during a series of screening visits described below. There were a total of eight visits spaced over a time period of 16 months, with four visits corresponding to AOSLO imaging, three visits corresponding to screening tests consisting of conventional clinical measures, and one visit corresponding to a routine FA. A summary of the visit dates is shown in Table 1. For all visits, the subject's left eye (OS) was selected.

After careful explanation of all study procedures, informed consent was obtained. All procedures were approved by the University of California, Berkeley Committee for Protection of Human Sub-

TABLE 1.
Visit information

	AOSLO visit 1	AOSLO visit 2	AOSLO visit 3	AOSLO visit 4
AOSLO date	10/21/2009	11/24/2009	7/6/2010	2/6/2011
Screening date	9/30/2009	—	4/27/2010[a]	1/30/2011
Screening result	Severe NPDR[b]	—	Severe NPDR	Severe NPDR[c]
HbA1c	9.8%	—	9.8%	10.8%
Visual acuity[d]	20/20	—	20/20	20/20
log CS[e]	1.50	—	1.50	1.50
Blood pressure[f]	125/74	—	116/74	126/62

[a]Fluorescein angiogram was performed on 5/28/2010.
[b]Severe non-proliferative diabetic retinopathy.
[c]Contralateral eye developed clinically significant macular edema.
[d]Snellen visual acuity.
[e]Contrast sensitivity.
[f]Blood pressure, left arm standing.

jects, and were in compliance with the World Medical Association's Declaration of Helsinki.

Screening Visits

Before three of the AOSLO visits, the subject was invited for additional screening to monitor the clinical progression of the patient's retinal health. Each screening visit was paired to one of the AOSLO visits. For the screening visits, the procedures listed in Table 1 were performed, as well as a medical history, spectral domain optical coherence tomography (SDOCT) (Cirrus HD-OCT Model 4000, Carl Zeiss Meditec, Dublin, CA), and color fundus photography (Zeiss Visucam Pro NM, Carl Zeiss Meditec, Dublin, CA). A 20° × 20° macular cube was acquired using the SDOCT. The fundus photograph was examined by a retina specialist to assess the grade of DR. The assessment was performed offsite with no information about the patient or disease history.

Between AOSLO visits 2 and 3, the patient developed clinically significant macular edema in the contralateral eye and was subsequently referred for a FA study. The FA was acquired using a digital fundus camera (Zeiss Visucam NM/FA, Carl Zeiss Meditec, Jena, Germany). Photos were acquired using standard protocols. The photo that most clearly showed the parafoveal capillaries in the left eye (OS) was selected for comparison to AOSLO imaging. To facilitate the comparison of AOSLO to FA, the FA was contrast-adjusted to best show the parafoveal capillaries. The goal of the comparison was to verify that capillaries and clinical features such as MAs could be properly identified.

AOSLO Visits

For the AOSLO visits, a series of overlapping videos were acquired near the foveal region of the retina. Individual photoreceptors could be resolved in the videos; the flow of individual leukocytes through retinal capillaries could also be seen. Videos were processed to generate high-contrast images of photoreceptors and capillaries. On the first visit, a series of overlapping videos were taken in the parafoveal region corresponding to approximately 5° in size, resulting in an image of the capillaries immediately outside the FAZ but not the surrounding capillary network. On subse-

quent visits, videos were taken in a region corresponding to approximately 10° in size, centered on the FAZ, along with additional videos centered on MAs and an IRMA. The videos were used to generate images of the FAZ and surrounding capillaries. AOSLO imaging was performed using parameters optimized for capillary imaging (40 s videos, 60 fps).[10] During video acquisition, the subject's pulse was simultaneously recorded.

We analyzed photoreceptors, capillaries, and leukocytes using the AOSLO videos. To analyze the photoreceptors, locations of individual cones were labeled, and cone spacing was quantified.[17,18] To assess the capillaries, the FAZ was extracted using a semiautomated procedure[5] and the diameter quantified to determine the precision with which FAZ size could be quantified. To evaluate whether there was capillary dropout in the parafoveal region, we quantified the total capillary perfusion length in a region of interest within 0.15° of the edge of the FAZ.[5] We analyzed the distribution and measured the speed of leukocytes across visits using spatiotemporal plot analysis.[10,19] Previously, we showed that a small subset of capillary channels called leukocyte-preferred paths (LPPs) account for a clear majority of leukocyte traffic.[10] However, it was uncertain whether the same LPPs would be identified on different visits, particularly in the presence of DR.

AOSLO images were compared across visits to detect structural changes in the capillary network, including any formation of new MAs or disappearance of existing MAs, as well as dropout of capillaries. The FAZ was also assessed to determine whether there were any changes.

RESULTS

Clinical Assessment

The patient was diagnosed with type 1 diabetes 20 years before his first visit, with no history of hypertension or hyperlipidemia. The SDOCT showed no clinically significant changes across visits: macular thickness was within normal limits and the IS/OS junction was intact (an abnormal junction would be indicative of photoreceptor disruption). For all visits, the retina specialist determined that the patient had severe NPDR. The retina specialist also assessed the FA study and determined that the patient had severe

NPDR based on identification of hemorrhages in four quadrants and IRMAs in two quadrants.[20] The HbA1c, visual acuity, contrast sensitivity, and blood pressure were also similar across the visits (Table 1). These tests show that the patient was stable as assessed by conventional clinical tests over all visits. The patient's refractive state was −0.25 D (correction required for retinal imaging) and axial length was 23.59 mm.

Detailed images of the vasculature were successfully generated using non-invasive AOSLO methods. Nearly all vessels seen in fundus photography and FA were also visualized using the AOSLO approach (Figs. 2 and 3).

Repeatability of AOSLO Imaging

Qualitatively, the same general structure of the capillary network was identified in each of the visits, with the exception of the fourth visit, where a single capillary dropped out, leading to a small increase in FAZ size (Fig. 4).

To quantify repeatability, the FAZ was extracted and the diameter quantified for all visits. The diameter was calculated as the diameter of the circle with equal area. Assuming that there was no change in the FAZ for the first three visits, we determined the 99% confidence interval for the FAZ diameter to be between 749 and 759 μm. The FAZ diameter on the fourth visit was 763 μm, a significant increase in size due to the dropout of a single capillary ($p < 0.01$).

Microaneurysms and Intraretinal Microvascular Abnormalities

Based on comparison to FA, the AOSLO was able to visualize MAs well. All the MAs identified on the FA could be identified in the AOSLO image from visit 3 (taken approximately 1 month later); there were some changes that could be identified when comparing these images with the other visits, which included development of a new MA and disappearance of an existing MA. There was also an object that appeared to be a multilobed MA (Fig. 5 and Supplemental Digital Content 2 available at http://links.lww.com/OPX/A88). One IRMA was imaged in visits 3 and 4 (Supplemental Digital Content 3 available at http://links.lww.com/OPX/A89). One of these micro-IRMAs developed a new capillary protrusion between visits 2 and 3, suggesting that these micro-IRMAs may be precursors to larger, clinically significant IRMAs.

Capillary Bends

A large number of capillary bends were observed using the AOSLO; such bends were visible but not clearly resolved by the FA (Fig. 6 and Supplemental Digital Content 4 available online at http://links.lww.com/OPX/A90).

Capillary Dropout

There was no uniform capillary dropout in the region of interest within 0.15° of the edge of the FAZ. The total capillary length per area was 33.94, 33.97, and 33.55 mm/mm² across visits 2, 3, and 4, which is within the range of capillary lengths measured in controls and patients with type 2 diabetes and no DR. In a previous study using the same AOSLO methods, we reported total capillary lengths per area of 33.45 ± 5.23 in controls and 31.43 ± 5.52 in patients with type 2 diabetes and no DR.[16]

Aside from the dropout of the capillary at the edge of the FAZ, there were also other areas of potential subclinical capillary dropout. In normal eyes, there are several capillary-free zones in the human retina that must be taken into consideration when identifying regions of capillary dropout. The largest capillary-free zone is the FAZ (in this patient, the FAZ had an area of 0.46 mm²). Near the FAZ, the capillary network is single-layered. Because capillaries are arranged in a circumferential manner around the FAZ, there are several rings of capillary-free zones called perifoveal intercapillary areas which correspond to this region of single-layered capillaries; the average area of these regions is approximately 0.001 mm² based on a previous study.[11] At larger eccentricities, one would not expect to find capillary-free zones of this size, except around arteries. There is a small capillary-free zone that surrounds arteries but not veins.[21]

There were two regions of capillary dropout (Fig. 7 and Supplemental Digital Content 5 available online at http://links.lww.com/OPX/A91). The first region was classified as a region of capillary dropout because of the size of the capillary-free zone. This region was located at an eccentricity too large to be a perifoveal intercapillary area, and the zone extended too far away from an artery to be a capillary-free zone from an artery (the areas of the regions of capillary dropout shown were between 0.020 and 0.022 mm²). Interestingly, this region was also a region where a MA disappeared. A second region of capillary dropout surrounded a vein, again at an eccentricity where there should have been multiple layers of capillaries.

Distribution and Speed of Leukocytes

Leukocytes were analyzed on visits 2, 3, and 4. For each visit, the capillary segments near the FAZ were identified and analyzed for leukocyte speed and frequency. A capillary segment was identified as a small capillary that featured single-file flow and no branching (i.e., all branching occurs upstream and downstream of the capillary segment). In total, 295 leukocytes were identified across all three visits. A histogram of leukocyte frequency was used to determine the set of capillaries that accounted for a clear majority of leukocyte traffic. These capillaries were called LPPs[10] (Fig. 8). In all three visits, the same four LPPs were identified; collectively, these LPPs accounted for 67, 62, and 68% of all leukocytes identified for visits 2, 3, and 4, respectively.

The speed of the leukocytes in each of the LPPs varied across visits, ranging from 1.24 to 1.97 mm/s (Fig. 9). Using the subject's pulse data recorded during video acquisition, leukocyte speeds were plotted vs. the cardiac cycle, averaged across the cardiac cycle, and then adjusted for differences in heart rate across visits 2, 3, and 4. To adjust for heart rate, speeds were multiplied by the scaling factor $R_2/R_\#$, where R_2 was the heart rate in visit 2 and $R_\#$ was the average heart rate in the visit number being assessed.

Assessment of Cone Photoreceptors

The same videos that were used to generate perfusion images were used to generate high-resolution images and montages of the cone mosaic. Cone spacing was assessed in various locations within
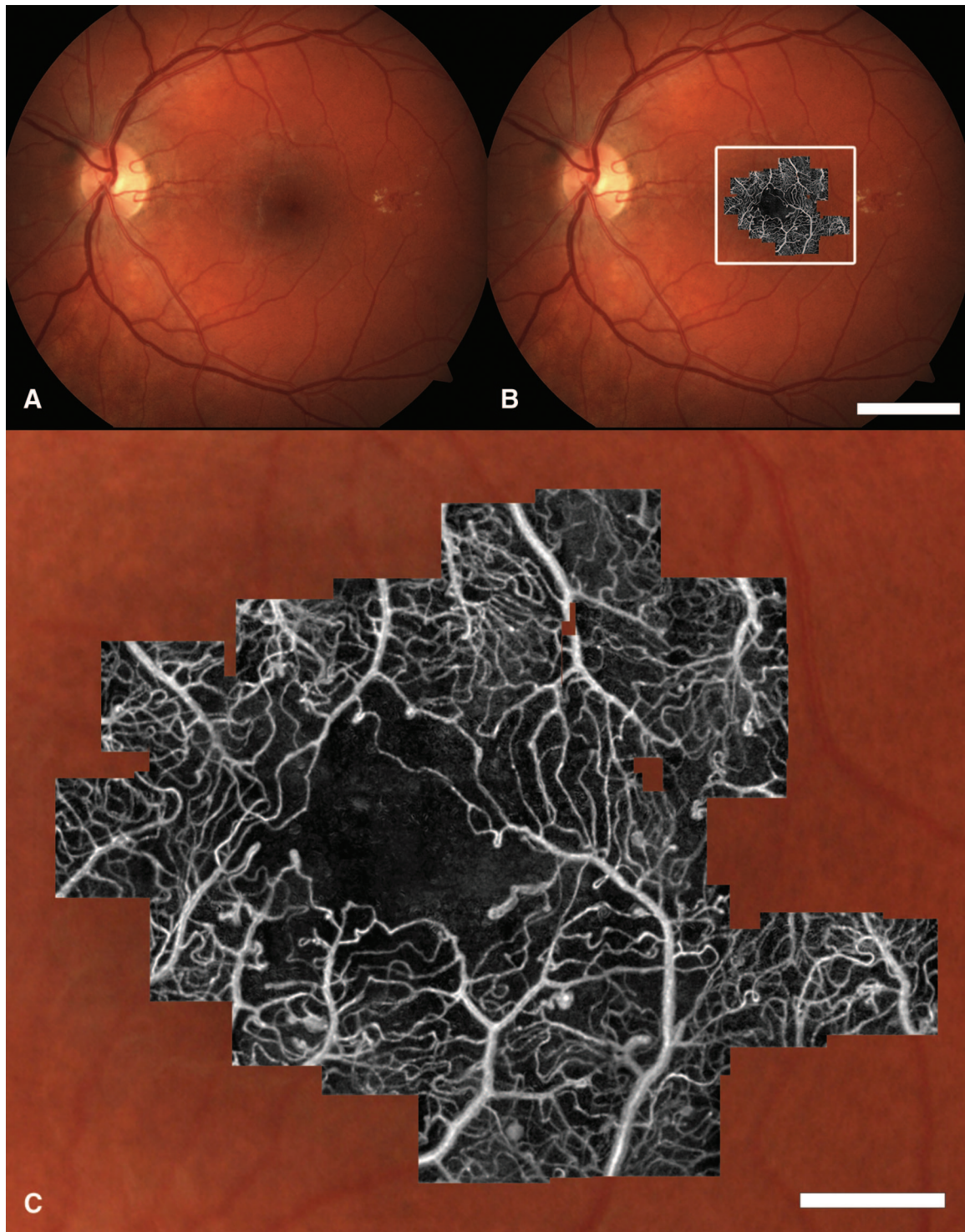
FIGURE 2.

Comparison of AOSLO imaging to color fundus photography. (A, B) Color fundus photo with and without the AOSLO image from visit 4. Scale bar, 2.5 mm. (C) Zoom of box from (B). A total of 43 overlapping AOSLO videos were combined to generate this image. In the center of the capillary network is a region free of capillaries called the foveal avascular zone (FAZ). Near the FAZ, microaneurysms and capillary bends can be seen. It is important to identify and monitor microaneurysms in patients with diabetes. Scale bar, 500 μm. A color version of this figure is available online at www.optvissci.com.

the montage for each visit. Spacing was estimated by manually selecting cone centers in contiguous unambiguous patches of cones and inferring the spacing from a histogram of all intercone distances within that set. Details on how cone spacing was estimated are reported elsewhere.[17,18] Cone spacing for each respective loca-tion was compared with expected spacing based on a database of 24 normal eyes (age range 20 to 40 years, average 25.6 years) that were imaged with an AOSLO and analyzed in the same manner as the current data. Our AOSLO spacing measurements on normal eyes[18,22] have been shown to compare well with histology.[23] An
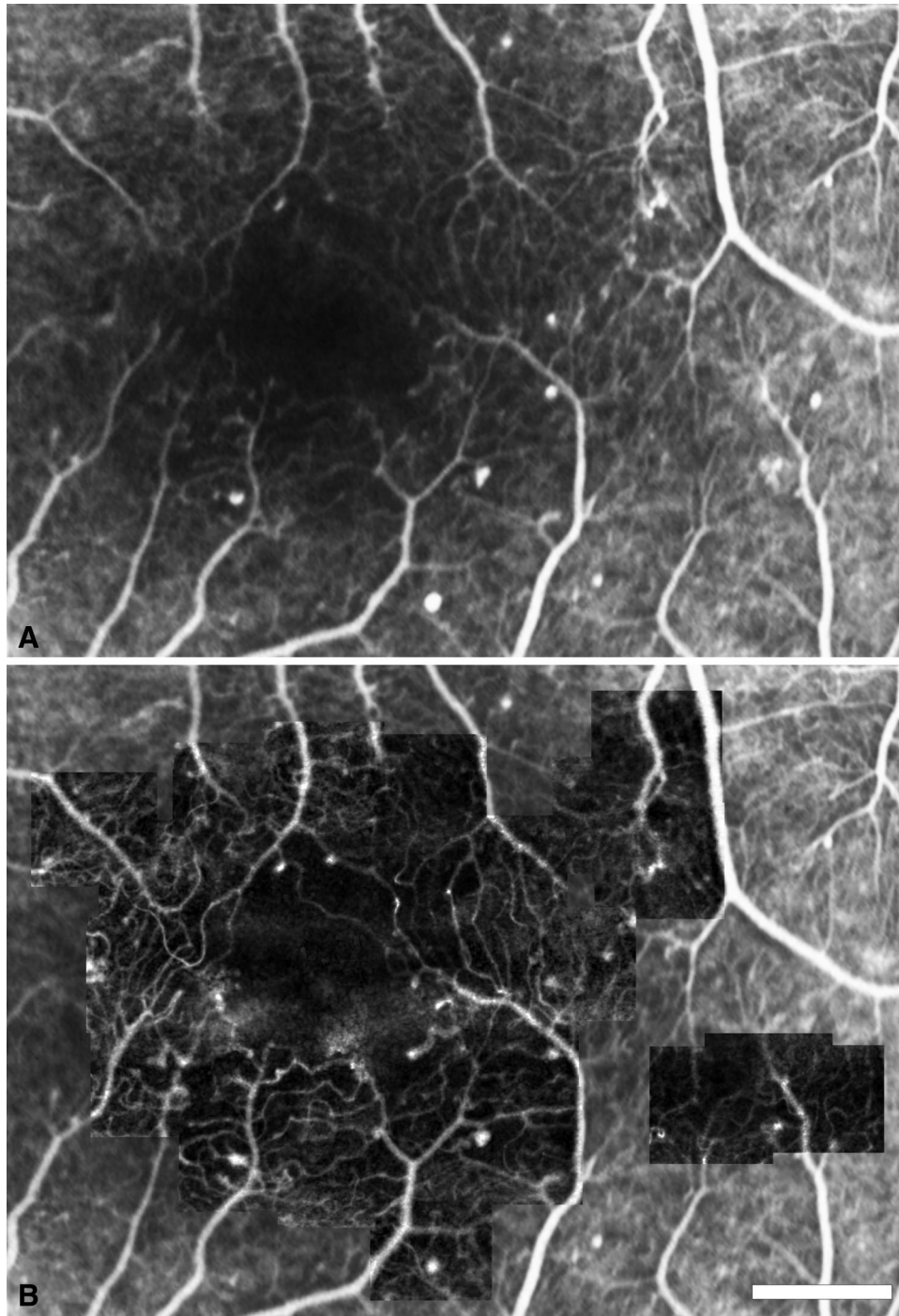
FIGURE 3.
Comparison of AOSLO imaging to fluorescein angiography (FA). The FA is contrast-adjusted for comparison purposes. (A) Capillaries and MAs as visualized using FA. A portion of the FA near the fovea is shown. (B) AOSLO image from visit 3 with the FA in the background. Scale bar, 500 μm.

exponential function fit was used to model the expected mean cone spacing with eccentricity:

$$spacing = A \times e^{-B\text{eccentricity}} + C$$

where A, B, and C are the constants. 95% Confidence intervals were determined to assess the range of normal spacing at each eccentricity. Deviations from normal were quantified as z-scores or the number of standard deviations from the normal mean at that location. In this particular patient, it was determined that cone spacing was normal (z-scores within ± 2), except in the fovea where cone spacing was higher than expected (i.e., cone density was lower than expected) (Fig. 10). The cone spacing at all locations within 250 μm of the foveal center was higher than the computed cone spacing of the normal eye with the lowest cone density in the histological study by Curcio et al.[23] as well as those reported in 18 normal eyes with varying eye lengths (from 22.86 to 28.31 mm) by Li et al.[22] The cone spacing measures were consistent between visits, and there were no signs of any progression over the four visits.
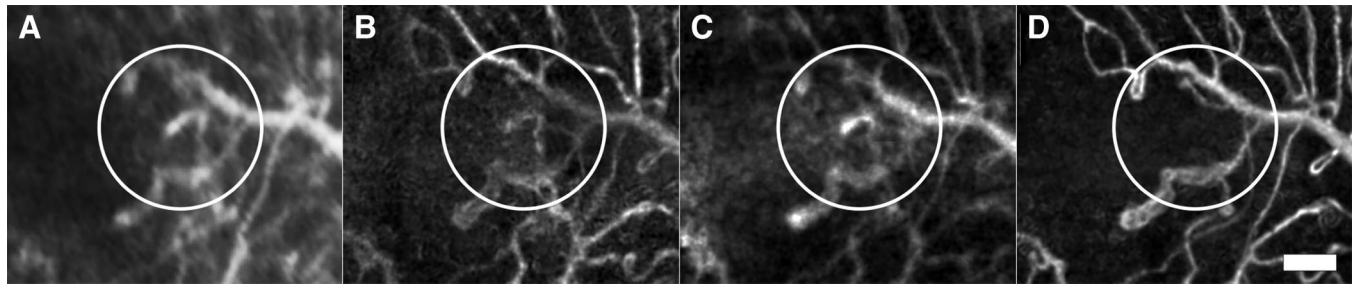
FIGURE 4.

Capillary dropout at the right edge of the FAZ. The same region on the retina is shown from the (A) fluorescein angiogram (FA), (B) visit 2, (C) visit 3, and (D) visit 4. Note that the FA was taken between visits 2 and 3. Scale bar, 100 μm.
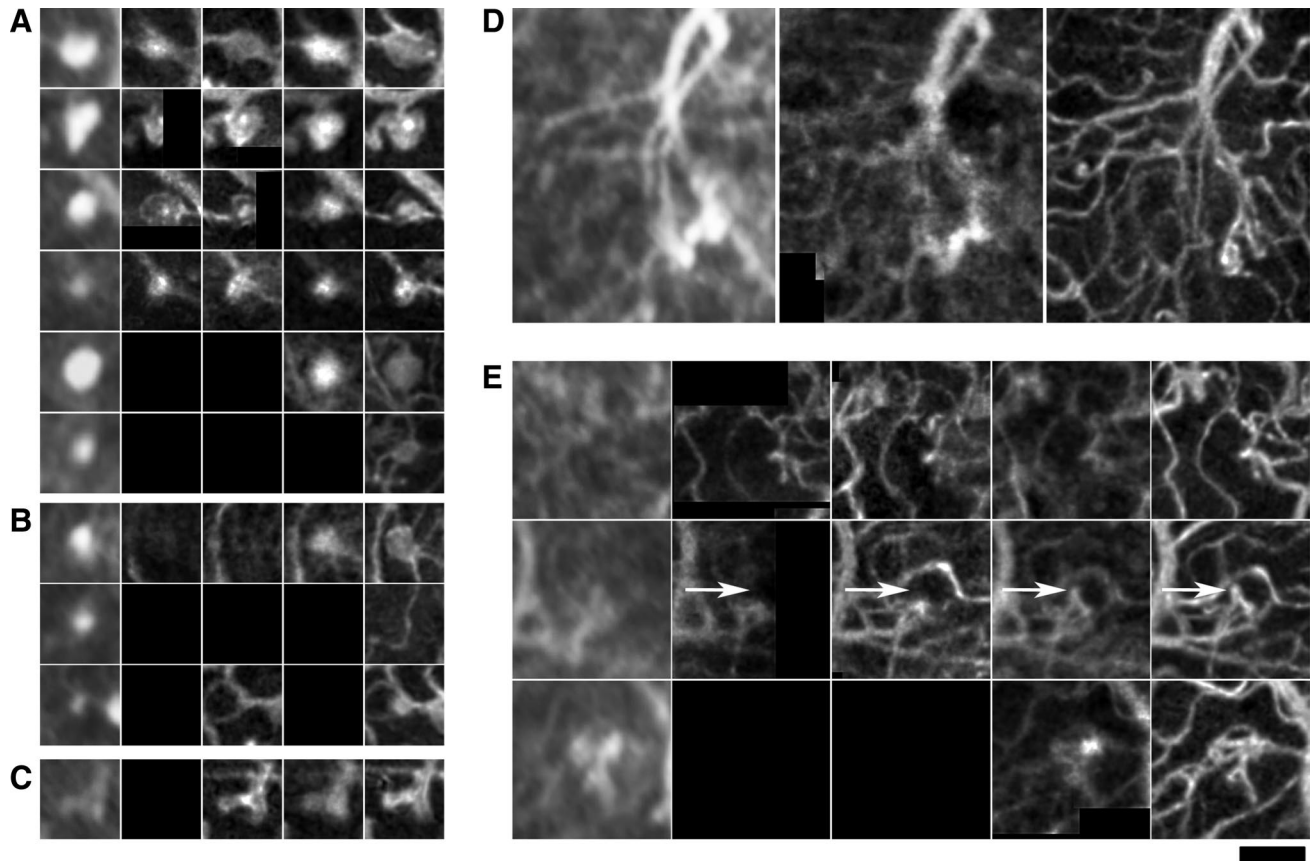

FIGURE 5.

Microaneurysms (MAs) and intraretinal microvascular abnormalities (IRMAs). Throughout the figure, only the first column shows images from the FA; the other columns show images from the AOSLO. (A, B, C) From left to right, the columns are images from fluorescein angiography (FA), visit 1, visit 2, visit 3, and visit 4. Black regions are areas that were not imaged by the AOSLO on that visit. The FA was performed between visits 2 and 3. FA panels are contrast-adjusted for better comparison to the AOSLO images (A) The same MAs could be seen across multiple visits. (B) There was one new MA which developed after visit 2 (top row) and one MA which disappeared between the FA and visit 4 (middle row). (C) MA-like object with two lobes. (D) One IRMA was identified. From left to right, the IRMA as seen by FA, visit 3, and visit 4. (E) Possible micro-IRMAs that were too small to be detected by FA. In one of the micro-IRMAs, a small capillary protrusion developed between visit 2 and the FA (arrow). Scale bar, 100 μm.

DISCUSSION

We show that AOSLO imaging can reliably image capillaries and capillary defects in NPDR on the basis of repeated application of AOSLO imaging alongside comparison to FA, the gold standard for visualizing human retinal capillaries. Subtle vascular changes occur even when the patient showed no changes in blood pressure, log CS, visual acuity, HbA1c, and DR severity as determined by graded fundus photographs (Table 1).

MAs are dynamic capillary defects spontaneously disappearing with an average half life of about 2 years for patients with type 1 diabetes and mild DR.[2] Of a total of nine MAs identified on the FA, we found one disappearance. However, given that we were restricted to the parafovea, we examined too few MAs to evaluate rates of MA appearance or disappearance. We found evidence of one MA increasing in size (Fig. 5B), which may suggest that MAs increase in size before disappearing. There was also one MA which disappeared (Figs. 5B and 7A). The region
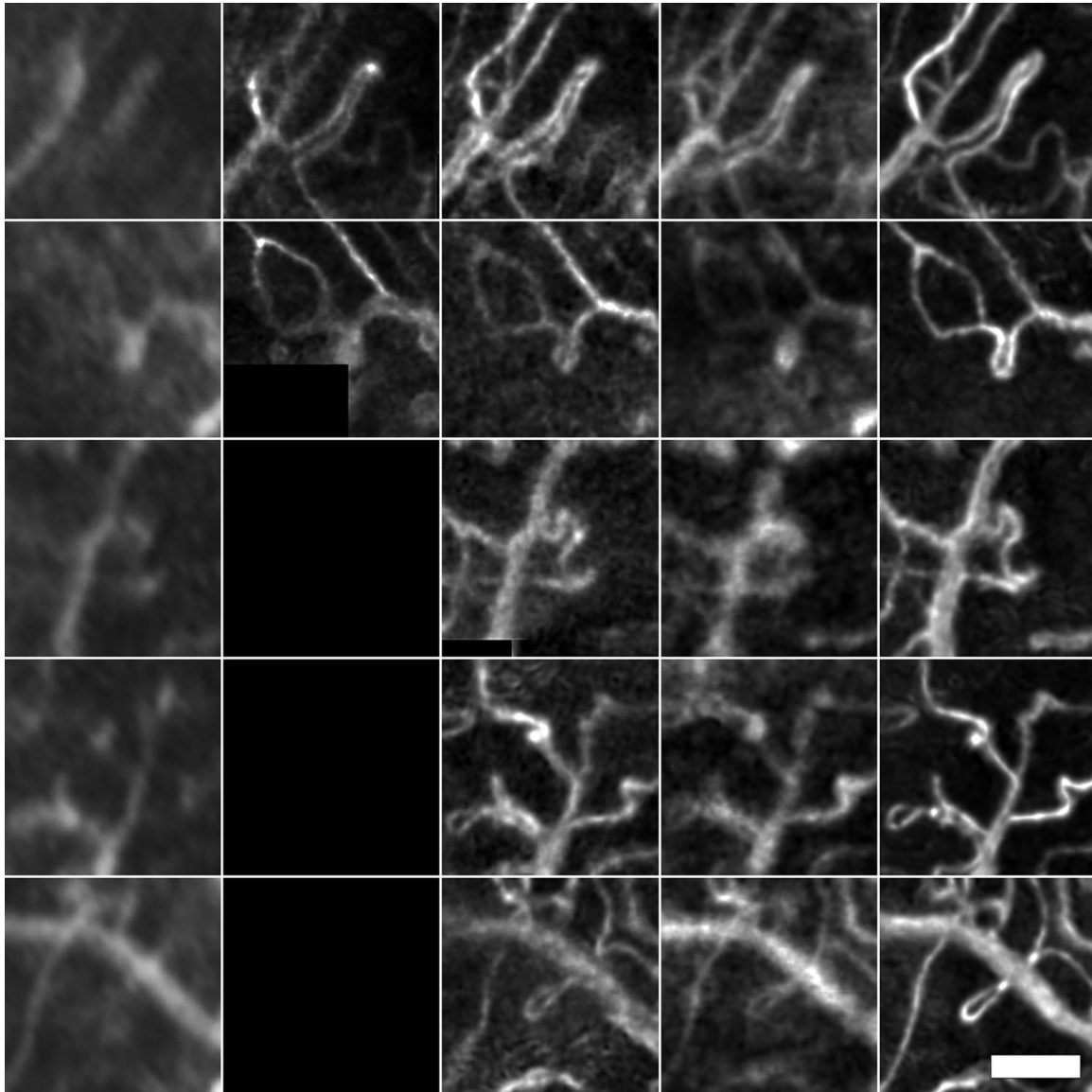
FIGURE 6.

Examples of capillary bends. Throughout the figure, only the first column shows images from the FA; the other columns show images from the AOSLO. The columns from left to right indicate images from fluorescein angiography (FA), visit 1, visit 2, visit 3, and visit 4. The FA was performed between visits 2 and 3. The FA was contrast-adjusted for better comparison to the AOSLO images. Scale bar, 100 μm.

near the MA disappearance is also one of capillary dropout, consistent with prior observations that MA disappearances are associated with capillary closure.[24] Disappearance of a MA is most likely due to thrombogenesis.[25] It has been suggested that thrombotic phenomenon in MA is facilitated by changes in erythrocyte and leukocyte flow through the capillaries.[24] In this eye, there are no LPPs in the supero-temporal region of the parafovea (Figs. 2 and 8). The absence of LPPs in this region could lead to a disruption of erythrocyte and leukocyte flow near that region; the location of the MA disappearance is in the supero-temporal region, although at a greater retinal eccentricity (Figs. 2C and 7A).

FAZ size is often used as a proxy for capillary dropout, with larger FAZs indicative of more serious levels of retinopathy.[26] Using the same AOSLO method described in this article, we measured FAZ diameters to be 584 ± 136 μm in controls and 627 ±

118 μm in patients with type 2 diabetes and no DR[16] (all numbers average ± standard deviation), compared with the measurements of 749 to 759 μm in this patient who had severe NPDR. These measurements are in agreement with prior studies of FAZ size using FA.[12,27,28] In these cross-sectional studies, it is assumed that increases in FAZ size are the direct consequence of capillary dropout. In this article, we perform longitudinal assessment on one subject, eliminating the confounding factor of intersubject variability, and show direct evidence of capillary dropout leading to an increase in FAZ size. Although the sensitivity of FAZ size as an imaging biomarker is limited due to large intersubject variability, noninvasive assessment of the FAZ may be important for longitudinal comparisons within the same patient (i.e., changes to the size of the FAZ in an individual may be more significant than the absolute size of the FAZ compared with a population). The AOSLO can be used to identify subtle events that cause the FAZ to
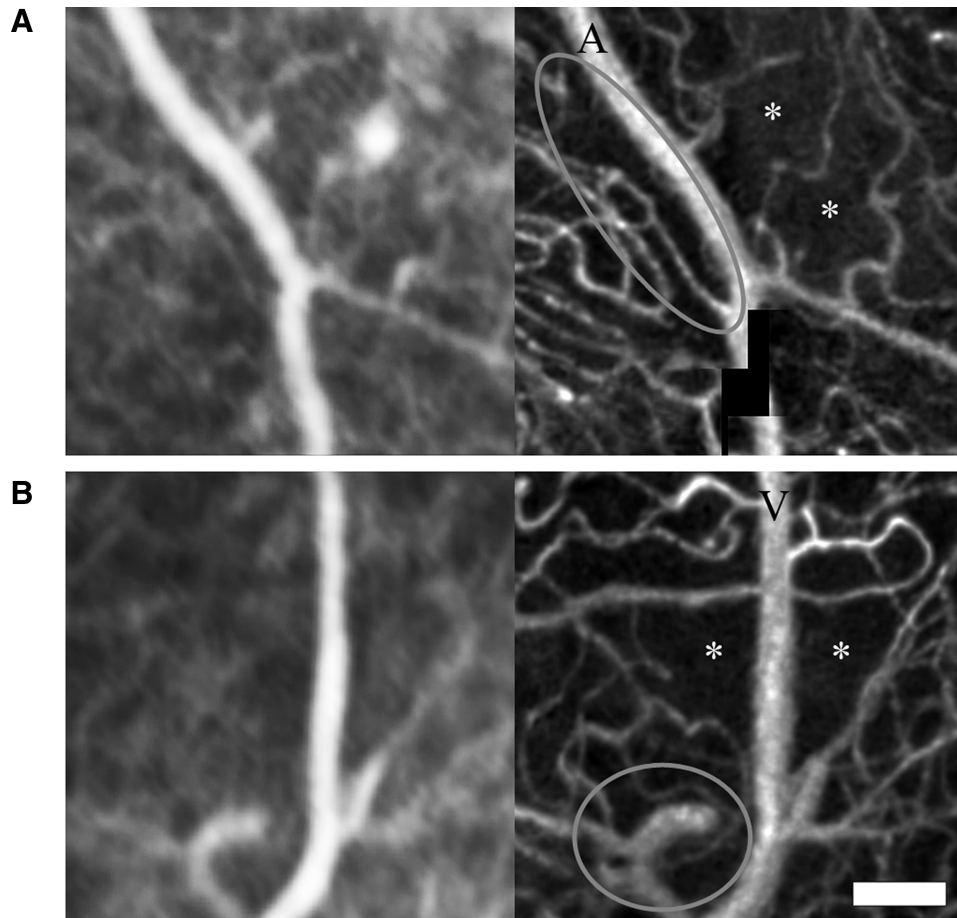
FIGURE 7.

Subclinical capillary dropout. Regions of capillary dropout are marked with an asterisk (*). Images are taken from the fluorescein angiogram (left) and the AOSLO on visit 4, approximately 8 months later (right). The fluorescein angiogram is contrast adjusted. (A) Two regions of capillary dropout next to an artery (A). The circled region is not considered to be capillary dropout as it is part of the capillary-free zone surrounding the artery. Note the disappearance of a microaneurysm at the area of capillary dropout. (B) Two regions of capillary dropout next to a vein (V). It is possible that additional capillaries dropped out between the time of the FA and the AOSLO imaging. A venous bend is circled. Scale bar, 100 μm.

increase in size. In this subject, we also show some areas of subclinical capillary dropout.

Leukocytes are involved in the development of DR.[29] However, the direct relationship between leukocytes and clinical signs of DR has not been shown in humans, due to the difficulty of assessing leukocytes in vivo. In this patient, we showed that the distribution of leukocytes in the capillaries near the FAZ is stable over a period of 15 months, even in the presence of small changes in the neighboring capillaries (Fig. 8). Leukocyte speed through LPP1 was consistently higher when compared with other LPPs. Thus, an important consideration for the interpretation of capillary speed measurements in any study is that the speed is dependent on the specific capillary that is being measured.

The state of cone photoreceptor spacing in DR is unknown and, unfortunately, we are not able to reach meaningful conclusions about photoreceptor spacing with one subject. The ability to image photoreceptors in live human subjects has only been enabled with recent advances in imaging technology. There is evidence of neural damage in DR,[30] suggesting that the photoreceptors may also be affected. However, in this patient, there was no evidence that the photoreceptor layers were disrupted in any of the SDOCT images. The increase in cone spacing observed by the AOSLO may be a

microscopic change that is too small to be detected by other methods. However, further studies are needed to answer this question and to further investigate the results presented in this article.

The main limitation of this study is that only one subject was assessed. Although the FA is of sufficient quality to visualize capillaries, it is by no means a representation of the highest quality FA that can be captured. Still, there is a large amount of data that can be quantified from the AOSLO videos, each consisting of 2400 video frames, enabling both static comparisons of vascular images and dynamic comparisons of leukocyte speed (as an example we quantified the speed of 295 leukocytes over three visits). Although no conclusions can be made about the natural progression of DR, there are several important clinical implications. First, we show that subtle capillary changes exist even when the patient appears to be stable. Such changes include the enlargement of an existing MA, development of IRMA-like capillary bends, and the dropout of a single capillary leading to the FAZ enlargement. Second, we show that the distribution of leukocytes traveling through the parafoveal capillary network is maintained over time, even in the presence of subtle changes in the neighboring capillaries. Moreover, we demonstrate the importance of specifying the capillary through which speed measurements are performed, as certain capillaries consis-
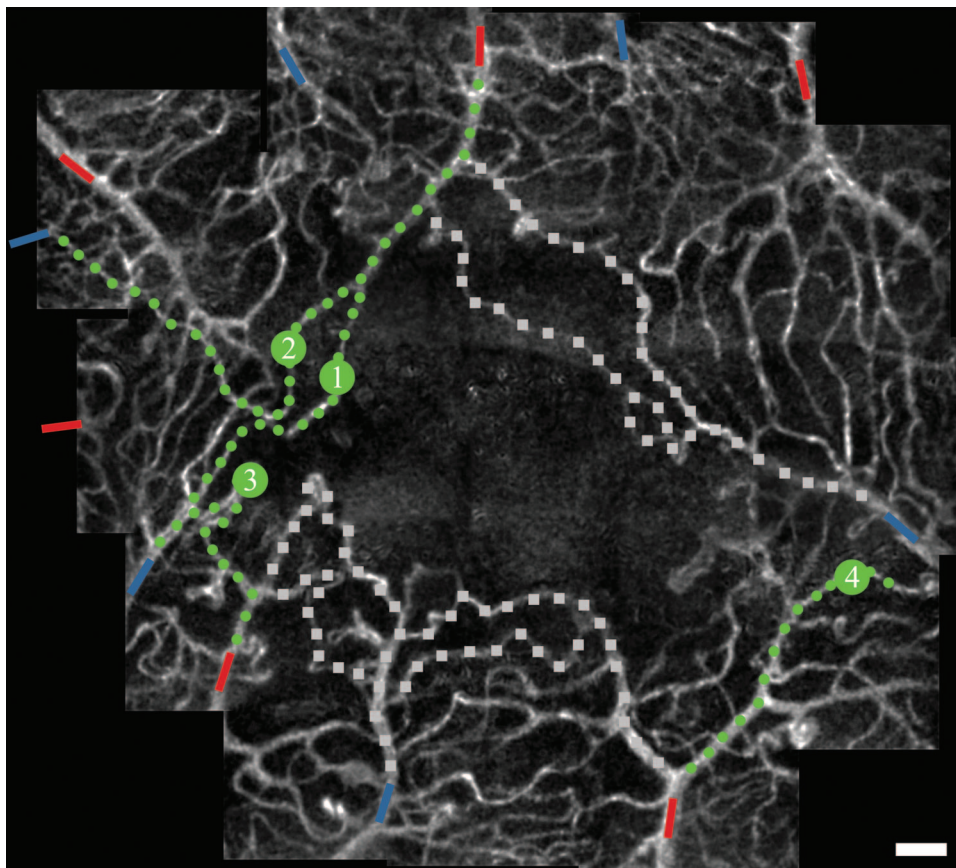
FIGURE 8.

Leukocyte-preferred paths (LPP) shown on the AOSLO image from visit 2. The same four LPPs were identified in visits 2, 3, and 4. Shown are capillaries identified as LPPs (green online) as well as capillaries which were assessed but not identified as LPPs (gray). Arterioles (red online) and venules (blue online) are shown for reference. Scale bar, 100 μm.
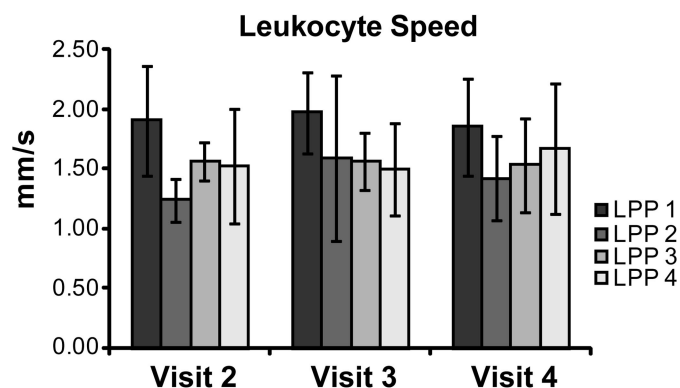

FIGURE 9.

Leukocyte speed. LPP 1, 2, 3, and 4 refer to the channels as labeled on Fig. 8. Speeds were averaged across the cardiac cycle and then normalized for heart rate. Error bars represent the standard deviation of the leukocyte speeds measured in the specified LPP and visit.

tently feature faster flow rates than other capillaries. Finally, we show that areas of focal capillary dropout exist, even when accounting for natural capillary-free zones in the parafoveal capillary network. These isolated areas may lead to the more widespread capillary dropout that is seen in the later stages of DR.

Simultaneous assessment of photoreceptors, capillaries, and leukocytes can potentially give rise to novel imaging biomarkers which could be used to monitor the progression of DR. Future work includes establishing a procedure for clinical interpretation of AOSLO images, because the sources of hyper- and hypointensity are different than what is conventionally expected. In the AOSLO images of capillaries, intensity is a measure of relative intensity fluctuation, with the assumption that intensity fluctuations are due to the motion of blood cells; the background photoreceptor tissue remains relatively stable in intensity when comparing neighboring frames of the video. It is unclear whether this variation in intensity contains useful information. Variation in intensity across distinct vessels can be attributed either to higher blood flow or to the fact that one vessel is closer to the plane of focus than the other vessel. In fact, the apparent diameter of a capillary is also dependent on its proximity to the plane of focus (see Supplemental Digital Content 3 available online at http://links.lww.com/OPX/A89), which is the reason why vessel diameters were not measured in this study. Within a single vessel, variations in intensity are most likely artifacts due to the presence of the underlying photoreceptor tissue. The quality of the AOSLO images varied over the visits due to continual modifications that were made to the AOSLO which is a custom-built research instrument. The image from visit 3 is out of focus, while the image from the final visit demonstrates results using a set of imaging parameters that are fully optimized for vascular imaging. Standardization of the technology will help ensure that the data quality is consistent
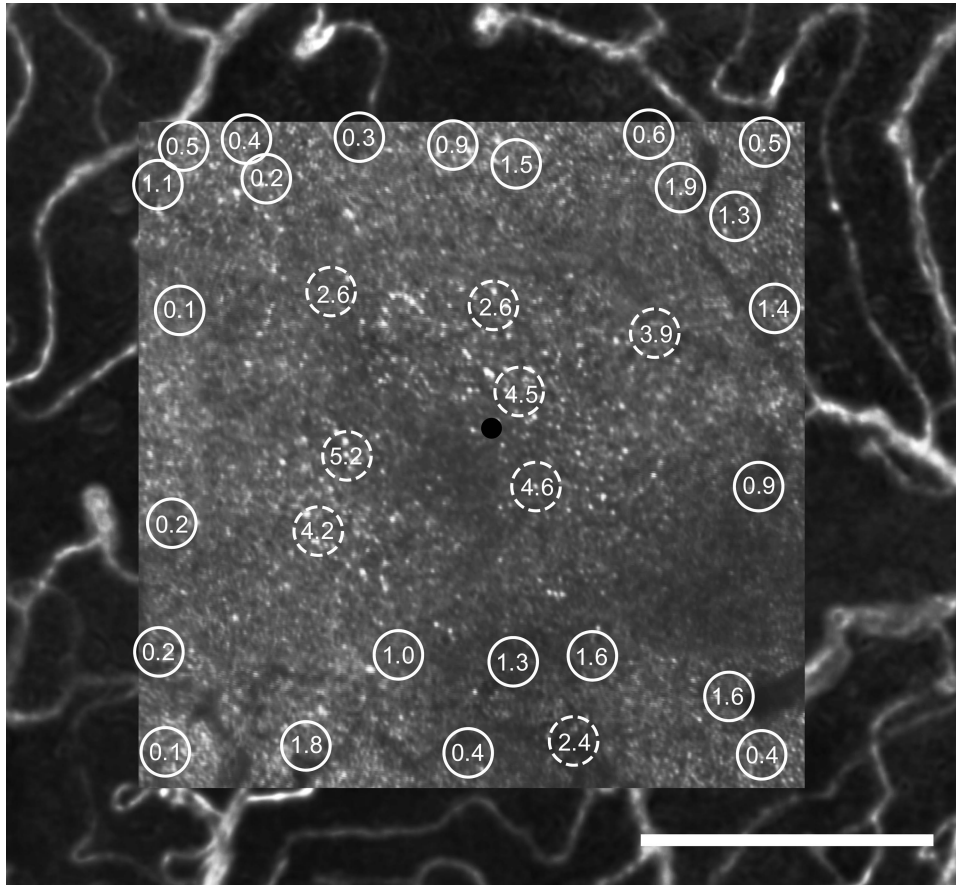
FIGURE 10.

AOSLO photoreceptor montage of the foveal region superimposed on top of the corresponding AOSLO perfusion image from visit 4. The black circle indicates the patient's preferred retinal locus for fixation. Cone spacing results are plotted as z-scores (number of standard deviations from the normal mean) at all locations where cone spacing was measured. Locations with z-scores >2 are indicated with dashed circles. Near fixation, cone density is decreased; further away from fixation, cone density returns to normal. Scale bar, 300 μm.

across visits. Despite these limitations, reproducible, detailed images of capillary features were successfully generated. Our results show that additional AOSLO studies involving patients with diabetes are warranted.

In conclusion, AOSLO imaging may give insights into how DR affects the photoreceptors, capillaries, and leukocytes. AOSLO imaging is repeatable and sensitive enough to detect changes such as the dropout of MAs and individual capillaries as well as the development of new MAs and IRMAs. The distribution of leukocytes seems to be unaffected by neighboring microvascular changes in the time course of 15 months. However, the relationships among the different vascular changes in DR are complex. Our results show that changes to the capillaries may occur even in the absence of clinically significant changes.

ACKNOWLEDGMENTS

SUPPLEMENTAL DIGITAL CONTENT

Supplemental Digital Content 1–5 are available online at http://links.lww.com/OPX/A87, http://links.lww.com/OPX/A88, http://links.lww.com/OPX/A89, http://links.lww.com/OPX/A90, and http://links.lww.com/OPX/A91.

REFERENCES

1. Klein R, Klein BE, Moss SE, Davis MD, DeMets DL. The Wisconsin epidemiologic study of diabetic retinopathy. II. Prevalence and risk of diabetic retinopathy when age at diagnosis is less than 30 years. Arch Ophthalmol 1984;102:520–6.
2. Hellstedt T, Immonen I. Disappearance and formation rates of microaneurysms in early diabetic retinopathy. Br J Ophthalmol 1996; 80:135–9.
3. Zhang Y, Poonja S, Roorda A. MEMS-based adaptive optics scanning laser ophthalmoscopy. Opt Lett 2006;31:1268–70.
4. Roorda A, Romero-Borja F, Donnelly W, III, Queener H, Hebert T,

Campbell M. Adaptive optics scanning laser ophthalmoscopy. Opt Express 2002;10:405–12.

5. Tam J, Martin JA, Roorda A. Noninvasive visualization and analysis of parafoveal capillaries in humans. Invest Ophthalmol Vis Sci 2010; 51:1691–8.

6. Nelson DA, Krupsky S, Pollack A, Aloni E, Belkin M, Vanzetta I, Rosner M, Grinvald A. Special report: noninvasive multi-parameter functional optical imaging of the eye. Ophthalmic Surg Lasers Imaging 2005;36:57–66.

7. Schmoll T, Singh AS, Blatter C, Schriefl S, Ahlers C, Schmidt-Erfurth U, Leitgeb RA. Imaging of the parafoveal capillary network and its integrity analysis using fractal dimension. Biomed Opt Express 2011;2:1159–68.

8. Kim DY, Fingler J, Zawadzki RJ, Park SS, Morse LS, Schwartz DM, Fraser SE, Werner JS. Noninvasive imaging of the foveal avascular zone with high-speed, phase-variance optical coherence tomography. Invest Ophthalmol Vis Sci 2012;53:85–92.

9. Zhong Z, Petrig BL, Qi X, Burns SA. In vivo measurement of erythrocyte velocity and retinal blood flow using adaptive optics scanning laser ophthalmoscopy. Opt Express 2008;16:12746–56.

10. Tam J, Tiruveedhula P, Roorda A. Characterization of single-file flow through human retinal parafoveal capillaries using an adaptive optics scanning laser ophthalmoscope. Biomed Opt Express 2011;2: 781–93.

11. Sander B, Larsen M, Engler C, Lund-Andersen H, Parving HH. Early changes in diabetic retinopathy: capillary loss and blood-retina barrier permeability in relation to metabolic control. Acta Ophthalmol (Copenh) 1994;72:553–9.

12. Arend O, Wolf S, Jung F, Bertram B, Postgens H, Toonen H, Reim M. Retinal microcirculation in patients with diabetes mellitus: dynamic and morphological analysis of perifoveal capillary network. Br J Ophthalmol 1991;75:514–8.

13. Arend O, Wolf S, Remky A, Sponsel WE, Harris A, Bertram B, Reim M. Perifoveal microcirculation with non-insulin-dependent diabetes mellitus. Graefes Arch Clin Exp Ophthalmol 1994;232:225–31.

14. Gray DC, Merigan W, Wolfing JI, Gee BP, Porter J, Dubra A, Twietmeyer TH, Ahamd K, Tumbar R, Reinholz F, Williams DR. In vivo fluorescence imaging of primate retinal ganglion cells and retinal pigment epithelial cells. Opt Express 2006;14:7144–58.

15. Kwan AS, Barry C, McAllister IL, Constable I. Fluorescein angiography and adverse drug reactions revisited: the Lions Eye experience. Clin Experiment Ophthalmol 2006;34:33–8.

16. Tam J, Dhamdhere KP, Tiruveedhula P, Manzanera S, Barez S, Bearse MA, Jr., Adams AJ, Roorda A. Disruption of the retinal parafoveal capillary network in type 2 diabetes before the onset of diabetic retinopathy. Invest Ophthalmol Vis Sci 2011;52:9257–66.

17. Rodieck RW. The density recovery profile: a method for the analysis of points in the plane applicable to retinal studies. Vis Neurosci 1991;6:95–111.

18. Duncan JL, Zhang Y, Gandhi J, Nakanishi C, Othman M, Branham KE, Swaroop A, Roorda A. High-resolution imaging with adaptive optics in patients with inherited retinal degeneration. Invest Ophthalmol Vis Sci 2007;48:3283–91.

19. Tam J, Roorda A. Speed quantification and tracking of moving objects in adaptive optics scanning laser ophthalmoscopy. J Biomed Opt 2011;16:036002.

20. Early Treatment Diabetic Retinopathy Study Research Group. Grading diabetic retinopathy from stereoscopic color fundus photographs—an extension of the modified Airlie House classification. ETDRS report number 10. Ophthalmology 1991;98:786–806.

21. Michaelson IC, Campbell ACP. The anatomy of the finer retinal vessels. Trans Ophthalmol Soc UK 1940;60:71–112.

22. Li KY, Tiruveedhula P, Roorda A. Intersubject variability of foveal cone photoreceptor density in relation to eye length. Invest Ophthalmol Vis Sci 2010;51:6858–67.

23. Curcio CA, Sloan KR, Kalina RE, Hendrickson AE. Human photoreceptor topography. J Comp Neurol 1990;292:497–523.

24. Cunha-Vaz J, Bernardes R. Nonproliferative retinopathy in diabetes type 2. Initial stages and characterization of phenotypes. Prog Retin Eye Res 2005;24:355–77.

25. Boeri D, Maiello M, Lorenzi M. Increased prevalence of microthromboses in retinal capillaries of diabetic individuals. Diabetes 2001;50: 1432–9.

26. Mansour AM, Schachat A, Bodiford G, Haymond R. Foveal avascular zone in diabetes mellitus. Retina 1993;13:125–8.

27. Conrath J, Giorgi R, Raccah D, Ridings B. Foveal avascular zone in diabetic retinopathy: quantitative vs qualitative assessment. Eye (Lond) 2005;19:322–6.

28. Bresnick GH, Condit R, Syrjala S, Palta M, Groo A, Korth K. Abnormalities of the foveal avascular zone in diabetic retinopathy. Arch Ophthalmol 1984;102:1286–93.

29. Chibber R, Ben-Mahmud BM, Chibber S, Kohner EM. Leukocytes in diabetic retinopathy. Curr Diabetes Rev 2007;3:3–14.

30. Barber AJ. A new view of diabetic retinopathy: a neurodegenerative disease of the eye. Prog Neuropsychopharmacol Biol Psychiatry 2003;27:283–90.

Austin Roorda
UC Berkeley School of Optometry
485 Minor Hall
Berkeley, CA 94720-2020
e-mail: aroorda@berkeley.edu